THREE-DIMENSIONAL AIRFLOW SIMULATION IN GRAIN STORAGE BINS

Oleg Khatchatourian
Regional University of Northwestern Rio Grande do Sul State, R. São Francisco, 501, Cx. P. 560, 98700-000, IJUÍ-RS-BRAZIL
olegkha@unijui.tche.br

Manuel O. Binelo
Regional University of Northwestern Rio Grande do Sul State, R. São Francisco, 501, Cx. P. 560, 98700-000, IJUÍ-RS-BRAZIL
mbinelo@yahoo.com.br

Nelson A. Toniazzo
Regional University of Northwestern Rio Grande do Sul State, R. São Francisco, 501, Cx. P. 560, 98700-000, IJUÍ-RS-BRAZIL
toniazzo@unijui.tche.br

Fabiane A. de Oliveira
Regional University of Northwestern Rio Grande do Sul State, R. São Francisco, 501, Cx. P. 560, 98700-000, IJUÍ-RS-BRAZIL
fabiane@unijui.tche.br

Abstract. *Most works on grain stores airflow simulation are related to two-dimensional or axisymmetric cases, although, this flow is usually three-dimensional. Even if the grain mass distribution is two-dimensional or axisymmetric, the airflow inlets in those grain stores do not satisfy these conditions. Besides, an aeration in large grain stores frequently is realized separately for different segments. In this work, a mathematical model and software were developed for three-dimensional airflow simulation on grain storage bins of high capacity, considering non-uniformity of the seeds mass. Software used Blender3d for geometry construction, which is a free software tool for 3D modeling. For mesh generation is used Netgen, a free software mesh generation tool. Software, written in ANSI C++, imports the mesh generated by Netgen, builds the finite element global matrix, taking account the boundary conditions, and solves the obtained linear system by the SOR method. To take account the model's non-linearity effects (related to the coefficient of pressure gradient permeability dependency on grain mass compression), the program executes an iterative process calculating the permeability coefficient distribution by the parameters obtained in the last iteration. To show the results graphically, the Paraview software is used, which is also free software. The simulations had shown good performance of the software developed, which can be applied to optimize the grain stores performance and to lower the engineering costs of new grain stores projects.*

Keywords*: Aeration, Mathematical modelling, Aerated grain storage, Finite-element method*

1. INTRODUCTION

Aeration, representing the forced air movement through a particulate medium formed by cereal grains, together with drying and sanitary phyto-control, is widely used to minimise crop losses after harvest. The purpose of aeration is the reduction and equalisation of temperature to create favourable conditions for product quality preservation during long periods of grain storage. The air, either blowing or aspirating, is distributed to cool the grain mass, to avoid humidity migration, to conserve the humid grains temporarily, to remove the scents of the stored grain mass and to apply fumigation.

The largest resistance to the airflow in an aeration system is caused by the grain mass. This resistance depends on the airflow parameters, on the characteristics of the surface of the product (rugosity), on the form and size of any extraneous impurity in the mass, on the configuration, and on the size of the interstitial space in the mass, on the size and amount of broken grains and on the product layer depth.

The works accomplished by Shedd (1953), Brooker (1961 and 1969), Brooker *et al*. (1982), Bunn and Hukill (1963), Pierce and Thompson (1975), Haque *et al*. (1981), Ribeiro *et al*. (1983), Maier *et al*. (1992), Khatchatourian and Toniazzo (1995), Weber (1995), Khatchatourian and Savicki (2004), and Khatchatourian and Oliveira (2006), examine the influence of some of these parameters on airflow pattern in seeds storage.

With increasing depth of grain storage, the grain mass can no longer be assumed as homogeneous. Non-homogeneity alters significantly the physical parameters involved in the aeration process, such as air velocity and static pressure drop. At the same time, there are no results in recent research related to the compaction factor of grain mass and the airflow pattern under these conditions.

To simulate the operation of the grain aerator with any type of air distribution systems, it is necessary to develop software for predicting the distribution of the parameters, because obtaining empirical data is a very difficult and costly task in these conditions. The principal objectives of the present work are:

(a) to create a mathematical model, an algorithm and software for the calculation of static pressure, streamlines and airflow velocity distribution in non-homogeneous conditions of air stream in 3-D aerated grain store;

(b) to determine the alteration of the compaction factor for several grain mass layer depths;

(c) to study the relationship between the air velocity and the pressure gradient as a function of the compaction factor;

(d) to incorporate the fan performance curve in the model; and

(e) to accomplish numerical simulations of actual and virtual aerated grain stores to detect the operational risk areas.

2. MATHEMATICAL MODEL

The problem of incompressible viscous isothermal flow is described by the system of equations of continuity (1) and of Navier-Stokes (2):

$$\mathrm{div}\,\mathbf{w} = 0 \tag{1}$$

$$\rho \frac{\mathrm{d}\mathbf{w}}{\mathrm{d}t} = -\mathrm{grad}P + \mu \nabla^2 \mathbf{w} \tag{2}$$

where: $\boldsymbol{w}$ is the velocity vector in m/s; ρ is the density in kg/m^3; t is the time in s; P is the pressure in Pa; μ is the dynamic viscosity in Pa s.

The solution of this system (usually reduced to the non-dimensional form) depends on the effective Reynolds number (calculated on apparent velocity taking into account the porosity of the grain mass) and relates the pressure and velocity distributions in each point of the integration domain for each moment in the form of a vector-function $\boldsymbol{w}=\boldsymbol{f}(\mathrm{grad}P)$, where the components u, v and w of velocity $\boldsymbol{w}$ and P are primitive variables of the initial system.

However, the experimental data show that even for the same Reynolds numbers Re for the airflow in the mass of several types of grains, the relationship between the velocity and the pressure gradient is different for each type of grain. This difference is probably caused by the factors that provoke variation of the airflow resistance: the geometrical form of the particles (which is not spherical and is distinct for different products), existence of porosity zones in the grain mass with limited air access (existence of two porosity types), distinction in the rugosity of particle surface, *etc*. There are many other factors, *e.g.*, grain layer compaction, variation of humidity content, presence of impurity in the mass, *etc.*, that increase the difference between the measured values and those calculated by the resolution of the system of Eq. (1) and Eq. (2). This fact implies that the attempts of simulating the airflow through the grain mass using the equations of continuity and Navier-Stokes in the form Eq. (1) and Eq. (2), contributing in theory, are far away from practical applications. The local air velocity in the aerated grain storage can vary in a wide range depending on the cross sectional area and on grain aerator design arrangement. Therefore, the grain storage can have domains of laminar, turbulent and transition flows. It essentially complicates creation of mathematical model and software, based on use of the Navier-Stokes equation.

For small velocities corresponding to laminar flow, a proportionality relationship exists between the air pressure drop and the air velocity (the formula of Hagen-Poiseuille or the equation of Blake-Kozeny):

$$\mathrm{d}P/\mathrm{d}y \sim |\mathbf{w}| \Rightarrow |\mathbf{w}| = k\,\mathrm{d}P/\mathrm{d}y \tag{3}$$

where, k is coefficient of proportionality.

Applying logarithms and taking the derivative:

$$\frac{\mathrm{d}(\ln|\mathbf{w}|)}{\mathrm{d}(\ln|gradP|)} = 1 \tag{4}$$

For the turbulent regime that corresponds to the larger values of air velocity the pressure drop is proportional to the velocity squared (equation of Burke-Plumer):

$$\mathrm{d}P/\mathrm{d}y \sim |\mathbf{w}|^2 \Rightarrow |\mathbf{w}| = k(|\mathrm{d}P/\mathrm{d}y|)^{1/2} \tag{5}$$

Similarly, for the turbulent regime:

$$\frac{\mathrm{d}(\ln|\mathbf{w}|)}{\mathrm{d}(\ln|\mathrm{d}P/\mathrm{d}y|)} = 0.5 \tag{6}$$

For a transition flow the relationship between the air pressure drop and the air velocity is intermediate between linear and square law dependence.

There are a large number of nonlinear motion equations in the literature to describe airflow in porous media. A review of many of them is presented in Scheidegger (1960), Bear (1988). In the majority of these equations the gradient of pressure is expressed as function of velocity by second-order parabola without a free term, *i.e.* as the sum of dependences for the laminar and turbulent regimes.

However it is difficult to describe precisely airflow by means of these formulas for all regimes (laminar, transition and turbulent flows). If coefficients in these formulas are chosen so that well to describe transition regime, influence of velocity in limiting situations (laminar or turbulent regime) will be too strong. If limiting regimes are well described, then dependence for transition regime is insufficiently exact. Moreover application of these formulas for cases 2-D and 3-D is difficult enough.

Khatchatourian and Savicki (2004) proposed the formula to describe the variation of the derivative d(ln|$\boldsymbol{w}$|)/d(ln(|dP/dy|)) for all the three flow conditions corresponding to the laminar, turbulent and transition flows:

$$\frac{\mathrm{d}\left(\ln|\mathbf{w}|\right)}{\mathrm{d}\left(\ln|gradP|\right)}=\frac{3}{4}-\frac{\arctan(U)}{2\pi} \tag{7}$$

where $U(P)=a\ln(|\text{grad }P|)+b$ is an intermediate argument; a>0 and b are constants.

Evidently, when $|\text{grad}P|\to 0$, $U\to-\infty$, $\lim\limits_{u\to-\infty}\left(3/4-\arctan(U)/2\pi\right)=1$, which corresponds to the laminar flow; and when $|\text{grad}P|\to\infty$, $U\to\infty$, $\lim\limits_{u\to\infty}\left(3/4-\arctan(U)/2\pi\right)=0.5$, which corresponds to the turbulent flow.

The numerical values of those derivatives represent the limit values of the derivative d(ln|$\boldsymbol{w}$|)/d(ln|grad$P$|) for variables |$\boldsymbol{w}$| and grad$P$ coupled by the function |$\boldsymbol{w}$| =f(|grad$P$|) in the total interval of variation |grad$P$|∈(0,∞) or ln|grad$P$|∈(-∞,∞).

Integrating Eq. (7) in relation to the logarithm of the pressure gradient, gives the expression for the velocity:

$$\ln|\mathbf{w}|=\left\{\left[\ln\left(1+U^2\right)-2U\arctan(U)\right]/\pi+3U\right\}/4a+c \tag{8}$$

where c is a constant of integration.

Finally, the mathematical model of the airflow in the particular media for the three-dimensional case consists of a system of two equations:

$$\operatorname{div}\mathbf{w}=0 \tag{9}$$

$$\mathbf{w}=-\frac{\text{grad}P}{|\text{grad}P|}\exp\left(\left\{\left[\ln\left(1+U^2\right)-2U\arctan(U)\right]/\pi+3U\right\}/4a+c\right) \tag{10}$$

The scalar Eq. (9) is the continuity equation for incompressible fluid. The vector Eq. (10) which has substituted the Navier-Stokes equation expresses that the velocity vector and pressure gradient are collinear in all points of the airflow domain and that the ratio of the modules of these vectors is a function of the pressure gradient.

Expressing the coefficient of proportionality k by:

$$k=\exp\left(\left\{\left[\ln\left(1+U^2\right)-2U\arctan(U)\right]/\pi+3U\right\}/4a+c\right)/|\text{grad}P| \tag{11}$$

and using Eq. (10), the velocity components u, v and w for the three-dimensional case can be expressed in the form:

$$u=-k\frac{\partial P}{\partial x};v=-k\frac{\partial P}{\partial y};w=-k\frac{\partial P}{\partial z} \tag{12}$$

where the y coordinate in m corresponds to vertical direction, the x and z coordinates are located in the perforated floor plan.

Substituting Eq. (12) in Eq. (9), the nonlinear partial differential equation is obtained:

$$\frac{\partial}{\partial x}\left(-k\frac{\partial P}{\partial x}\right)+\frac{\partial}{\partial y}\left(-k\frac{\partial P}{\partial y}\right)+\frac{\partial}{\partial z}\left(-k\frac{\partial P}{\partial z}\right)=0 \tag{13}$$

The boundary conditions for the problem considered have the form:

$P=P_e$ (Dirichlet condition for air entrance and exit) (14)

$\boldsymbol{n}\cdot\mathrm{grad}P = 0$ (Neumann condition on the walls and floor of the silo) (15)

where P_e is air entrance or exit pressure in Pa; and $\boldsymbol{n}$ is unit vector normal to the wall or floor surface.

Equations (11), (12) and (13) with the boundary conditions (14) and (15) describe a steady-state pressure and velocity distributions in a cross section of the aerated grain storage.

3. SOFTWARE DESCRIPTION

The resultant nonlinear partial differential equation for pressure (13) was solved by the finite element method (Segerlind, 1976) with an iterative process for the calculation of the permeability coefficient k by Eq. (11) in each point of the domain of integration, using the pressure distribution in the immediately previous iteration step.

The software developed in ANSI C++ consists of tools for geometry construction, mesh generation, generator of system matrix, solver of obtained system of linear algebraic equations and tool for results three-dimensional presentation and analysis. Because commercial tools have high costs, therefore free softwares were used when it was possible.

3.1. Geometry construction

For geometry construction was used Blender3D, available at http://www.blender3d.org. It is free software under GPL license. This tool is a 3-D modeler aimed to artistic works, but it proved to be very efficient for 3-D geometry construction of storage bins.

The data corresponded to storage bin geometry were exported to smash file format, which one can be read by Tetgen. It was modified a Perl script used for data exporting adding the exportation of face materials. To recognize the surfaces with different bounding conditions, such as inlets and outlets, for example, they were conditionally marked out as surfaces of distinct materials.

3.2. Mesh generation

For mesh generation Tetgen was used, available at http://tetgen.berlios.de/index.html, also under GPL license. It generates quality tetrahedral meshes using Delaunay algorithms. First a coarser mesh was generated. Initially, to refine the obtained mesh, a quality mesh file was generated by the solver, then, Tetgen itself was used to refine the mesh according to the parameters indicated in this file. But better results were obtained by dynamical adaptive refinement of the mesh based on the tetrahedron size per pressure gradient ratio. Each tetrahedral, which not satisfies the user specified ratio, is recursively decomposed in eight new tetrahedral elements according to the method shown at Liu and Joe (1996).

3.3. Problem solving and representation

A software was developed in this work for generation and solution of the system of linear algebraic equations. The developed software is cross-platform and can be compiled in cygwin on Windows, GCC on POSIX platforms, or any other ANSI C++ compatible compiler. The input files to solving software are the output files from Tetgen representing nodes, faces and tetrahedral elements, and also a file describing the boundary conditions and precision requirements. First the solving software generates the local matrix for each tetrahedron applying the finite element method. Using the information of the local matrices, the global system matrix is generated. Since the order of this system is large and the matrix is very sparse, a special class was created to handle the matrix, optimizing memory and also optimizing the access time to elements. In-house programming of special class instead of use of other standard sparse matrix classes permitted to take full advantage of system peculiarities, optimizing memory use and processor time. The Successive Overrelaxation Method (SOR method) was used for solution of system. The solver showed good performance.

Software executes three iterative processes: 1) to calculate the permeability coefficient in each point of the domain of integration, using the pressure distribution in the immediately previous iteration step, 2) to search the system design point, located in the performance curve of the aerator fan, and 3) to adaptively refine the mesh according to the tetrahedron size per pressure gradient ratio.

After the system is solved, an output file is generated in GTK format. This file includes the nodes and tetrahedral elements. For each node is exported the value of pressure, for each tetrahedral is exported the velocity vector. For results visualization Paraview software was used http://www.paraview.org, which is open source and available free of charge. Paraview has strong tools for CFD analysis and all images presented in this article were generated by it.

4. VALIDATION OF THE MATHEMATICAL MODEL FOR NON-HOMOGENEOUS CONDITIONS IN THE GRAIN MASS

To validate the proposed mathematical model, the empirical relationships between airflow velocity and static pressure drop were obtained for compacted layers of several grain storage depths. The coefficients *a*, *b* and *c* presented at the mathematical model for airflow through mass of divers types of grains (soya bean, corn, rice, oats and wheat) were obtained experimentally. In large storage bins, due to the compaction effect, the grain mass constitutes a non-homogeneous medium and the permeability coefficient varies as a function of the grain layer depth. In this work, the influence was studied of the grain mass compaction factor caused by the weight of the grain itself.

4.1. Experimental equipment

To simulate the characteristics of aerated grain storage, the equipment, described by Khatchatourian and Savicki (2004), was used to determine, experimentally, the grain mass compaction factor, due to the weight of superior layers. The grain mass porosity variation as a function of the layer depth and the compaction influence on the relationship between the airflow velocity and the static pressure drop were analysed.

Figure 1 presents the experimental equipment which consists of a centrifugal fan, an orifice-plate and small 'silo' composed of a polyvinyl chloride tube (diameter of 0.2 m and height of 1 m). To model the conditions at the bottom of a grain store, a compacting device was developed with a lever, which made it possible to apply moderate forces to simulate the depth up to 50 m.

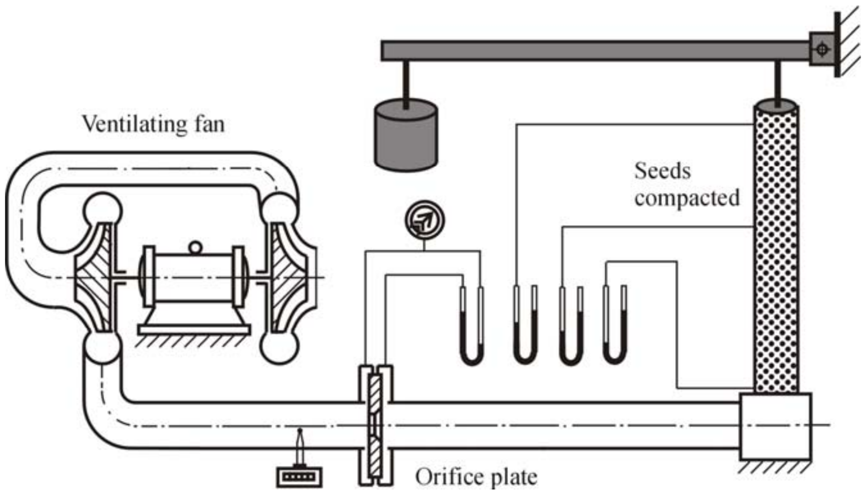

Figure 1. Sketch of the experimental equipment

In the tests, soya beans , corn, rice, oats and wheat were used, with a moisture content of 12-13% and impurity less than 2%, determined in the Laboratory of Analysis of Seeds of the Department of Agrarian Studies of the Regional University of the Northwest of the State of Rio Grande do Sul - UNIJUI.

4.2. Experimental results

The experimental results, presented in Fig. 2, establish dependence between airflow velocity and static pressure drop in the soya beans, maize, rice and wheat mass. Table 1 shows the values of empirical model coefficients *a*, *b* and *c*, obtained by minimization of discrepancy between experimental and simulated data. To reduce a number of different parameters, value of *a* for all seed types has been chosen identical, corresponding to value found for soya bean.

The simulations (curves in Fig. 2) based on this coefficients describe satisfactory the experimental data (the points in Fig. 2).

Experimental data (Fig. 3) show the significant influence of the depth of the storage layer on aerodynamic resistance of the mass in the studied interval (of 1 m up to 50 m). The analysis of the measurements of the porosity factor ε for various storage layer depths indicated that the sole consideration of the effective velocity increase due to the porosity factor reduction in the deepest layers is not enough to explain and calculate the pressure losses under these conditions.

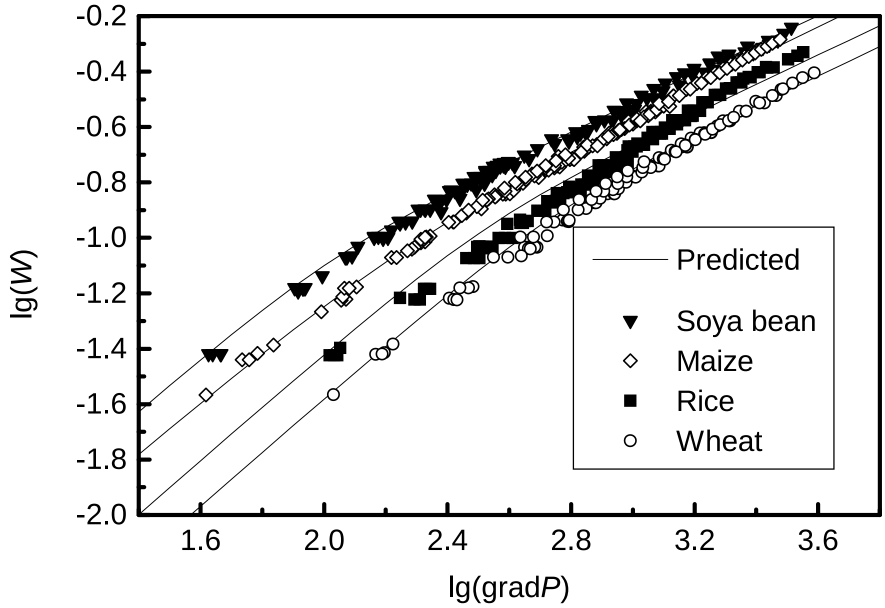

Figure 2. Relationship between air velocity (W) in m/s and air pressure drop (dP/dy) in Pa m^{-1}

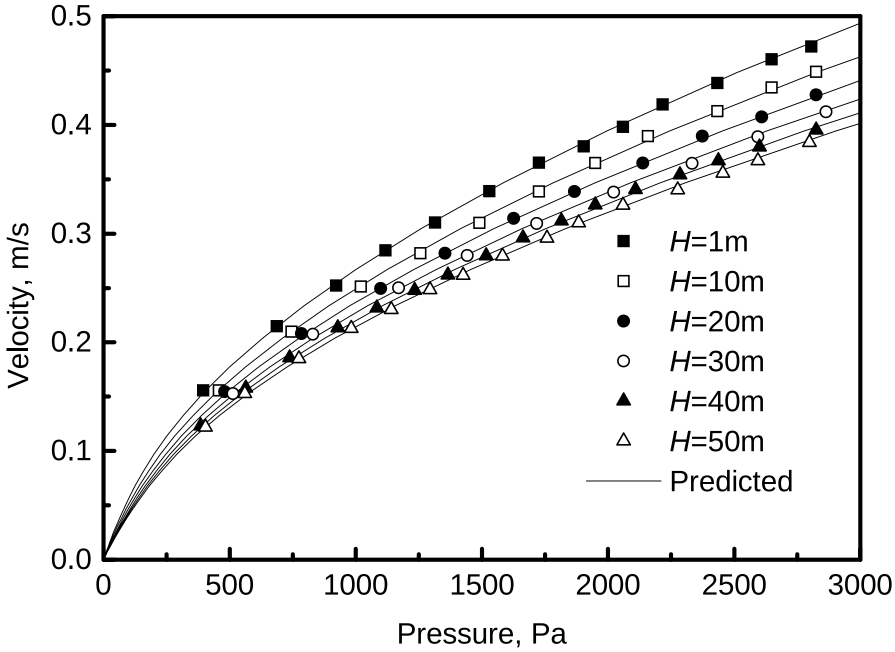

Figure 3. Influence of the grain mass layer depth (*H*) on the air velocity (*W*) in m/s (one-dimensional storage) as function of air pressure drop (d*P*/d*y*)

Table 1. Empiric coefficients *a*, *b* e *c* for different seed types.

Seed type	a	b	c
Soya bean	2.5	-5.0	-1.1
Maize	2.5	-5.56	-1.07
Rice	2.5	-6.2	-1.02
Wheat	2.5	-6.8	-0.94

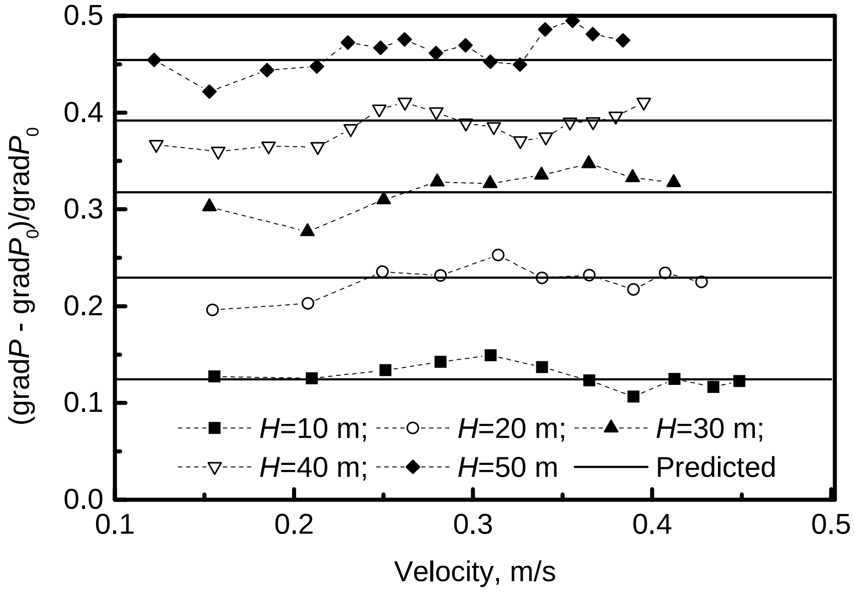

Figure 4. The variation of the relative pressure gradient *c* with maize layer depth at various air velocities

The experimental data, presented in Fig. 4, reveal that for the studied velocity and depth variation intervals, the relative pressure gradient increment $C = \left(\left|\text{grad}P_H\right| - \left|\text{grad}P_0\right|\right)/\left|\text{grad}P_0\right|$ can be considered independent of air velocity, depending only on storage layer depth *H*, where *H* is a distance in m between the upper seeds surface (free surface) and considered layer.

The function *C*=*C*(*H*) relates the initial pressure gradient module $\left|\text{grad}P_H\right|$, where P_0 corresponds to grain depth *H*=1 m, and the pressure gradient module $\left|\text{grad}P_H\right|$ for considered depth *H*. This function named in this work the compaction function, was presented in the form:

$$C(H) = G\left(1 - e^{qH}\right) \tag{17}$$

where *G* and *q* are empiric constants.
These empiric constants were obtained by minimizing of functional:

$$\min_{G,q} \sum_{i=1}^{M} \left| \frac{G\left(1 - e^{qH}\right)\text{grad}P_0}{\text{grad}P_i - \text{grad}P_0} - 1 \right| \tag{18}$$

where *M* is total number of experimental points for selected grain type.

Table 2. Empiric coefficients of compaction function for different seed types.

Seed type	*G*	*q*
Soya bean	0.68	-0.037
Maize	0.788	-0.0172
Rice	0.782	-0.0165

The compaction function allowed the inclusion of the influence of the depth *H* in the model through the intermediate argument *U*, substituting the pressure gradient without compaction $\left|\text{grad}P_0\right|$ for the expression $\left|\text{grad}P_H\right|/(1+C)$:

$$U = a\ln\left(\left|\text{grad}P_H\right|/(1+C)\right) + b \tag{19}$$

As a result, Eq. (8), with Eq. (17) and with the intermediate argument in Eq. (19), relates the requested air velocity for the storage layer located in the depth *H*, and the necessary pressure gradient. The calculated curves describe satisfactorily the experimental data (Fig. 3 and Fig. 4).

To simulate the storage bins of complex layouts, the software was completed by an iterative process which determines equilibrium between the fan output and the resistance of the aeration system to airflow, *i.e.*, the operating point of the aerator fan. Then, the software solves the problems: (1) calculation of the necessary pressure to get the required airflow rate (estimating static pressure requirements); (2) calculation of the airflow rate, knowing the initial pressure; and (3) calculation of the pressure and airflow rate in an iterative process for the chosen fan and electric motor (estimating system design point).

5. NUMERICAL SIMULATIONS

Figure 5 shows the structural layout of real V-form floor storage bin, used in the state of Rio Grande do Sul (Brazil). The storage bin presents a maximum width of 30 m and length of 95 m. Three air inlet systems were analysed: 1) central inlet system; 2) central and upper lateral inlet system; and 3) central, lower lateral and upper lateral inlet system. The aeration simulations in storage bins, for different layouts, were generated using the airflow rate of 9 $m^3h^{-1}t^{-1}$ (2.5×10^{-6} m^3s^{-1} kg^{-1}), which is the most recommended values in aerated grain storage. The pressure value in lower lateral inlet constituted 50% of central inlet pressure and in upper lateral inlet 25%.

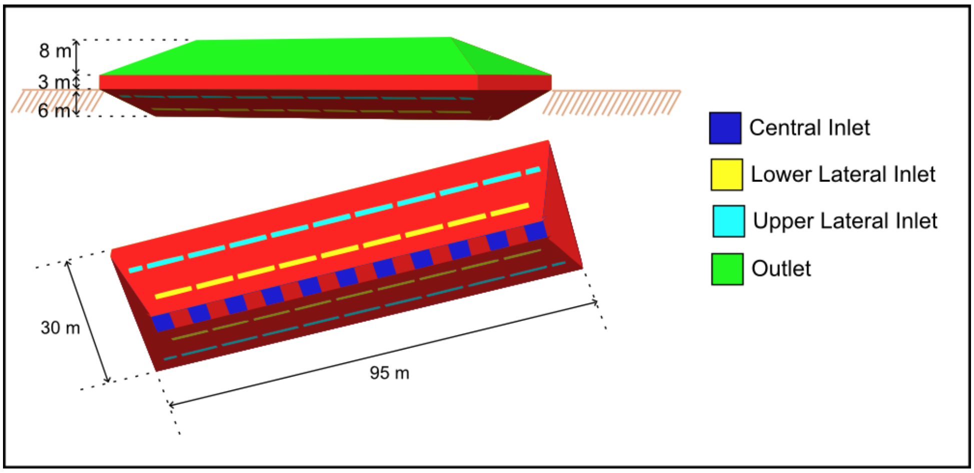

Figure 5. Outline sketch of simulated store bin

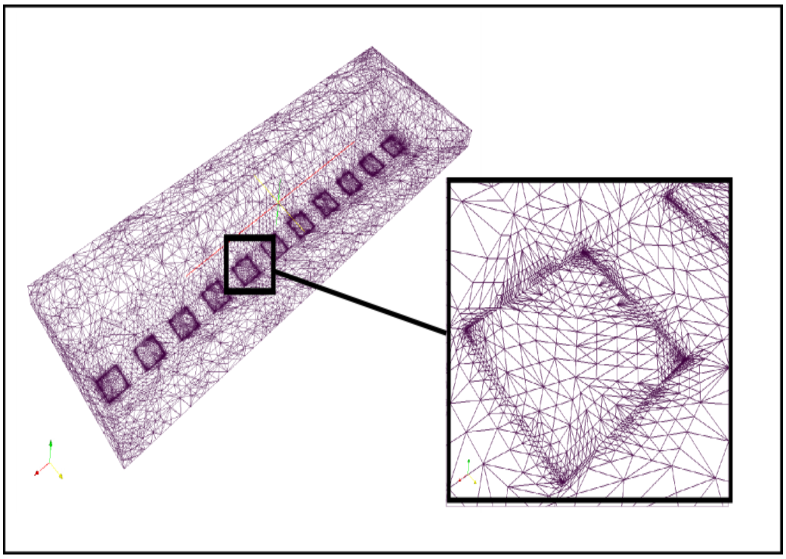

Figure 6. Surface wireframe of the tetrahedral mesh

First, airflow simulation in the V-form floor storage bin was made for case 1 (air inlet ducts installed in the base of the storage). Although in considerate case the storage bin has two symmetry axes and it is possible to consider solely ¼ of total storage, the simulation was realized for complete domain, because in general case the symmetry condition does not exist.

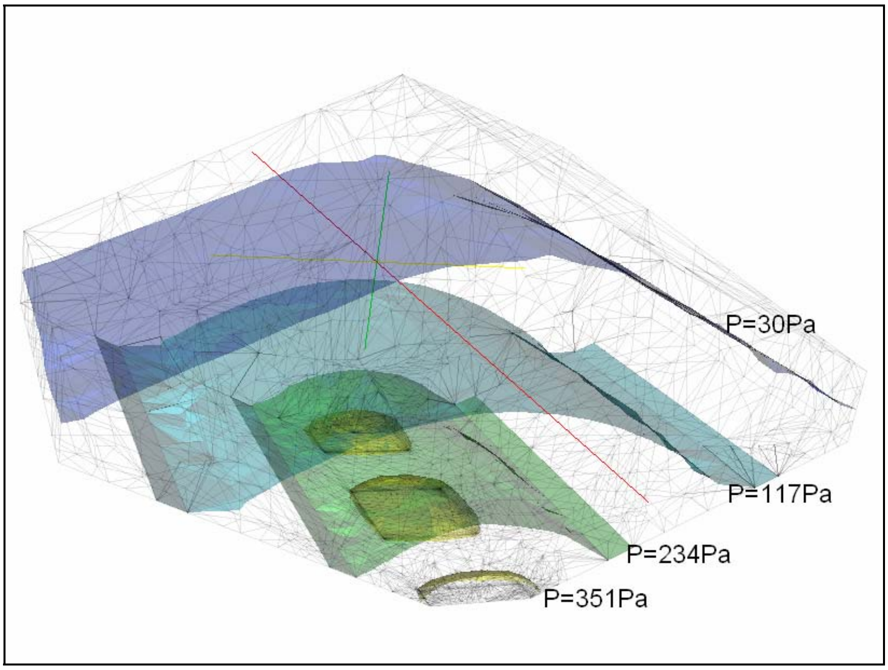

Figure 7. Isobar surfaces in storage bin section with central, lower lateral and upper lateral inlet system

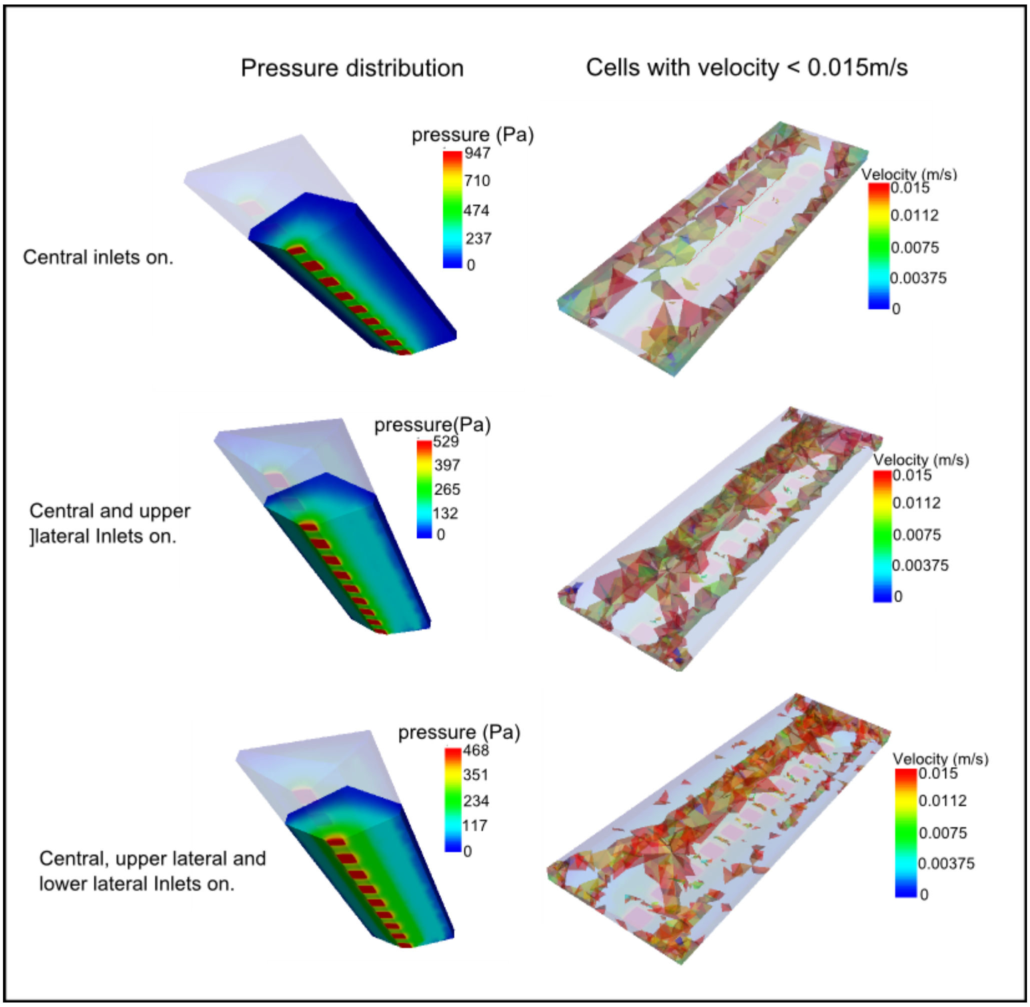

Figure 8. Comparison of three simulated aeration systems: distribution of pressure (left column) and risk domains (right column)

Figure 6 presents the part of computational mesh used. Grid has major density in domains where modulo of the pressure gradient is major. For considered layout the number of tetrahedrons is approximately equal of 500.000.

Isobar surfaces for storage bin section with central, lower lateral and upper lateral inlet system are showed in Fig. 7. It could be seen that airflow in lower storage part has essentially 3-D character. In upper storage part, an airflow character approaches 2-D case.

The results of simulation of three considered aeration systems are presented in Fig. 8. Analysis of pressure distribution (left column) showed that the installation of lateral ducts equalised essentially the airflow in comparison with the same storage bin without lateral ducts and reduces initial pressure head. To visualize risk domains, software permits to show the storage parts, which satisfy the certain conditions. For example, the frameworks in Fig. 8 (right column) present only cells with velocity less than 0.015 m/s, *i.e*., the domains with reduced aeration capacity.

The system with central, lower lateral and upper lateral inlets on has considerably improved conditions of storage in domains close to walls in comparison with other considered outlets. For all considered cases there is an area of risk in the uppermost part of grain mass.

6. CONCLUSIONS

1) A mathematical model of 3-D airflow in an aerated grain storage system was developed for non-uniform conditions of the seed mass.

2) Experiments were conducted to obtain the relationship between air velocity and pressure gradient and the values of the porosity factors for different seed type and different storage layer depths.

3) Software was elaborated to determine the airflow rate and initial pressure head in the grain mass store for the chosen fan and electric motor for 3-D case.

4) Experiments and numerical simulations showed the need to consider the non-uniformity of the grain mass in seed storage, in order to choose the estimated performance of the aeration system.

5) The aeration system efficiency of several seed storages was analysed (the airflow distribution uniformity and the static pressure head values to generate the appropriate airflow rate for safe storage).

7. REFERENCES

Bear, J., 1988, "Dynamics of Fluids in Porous Media", Dover Publications, New York.

Brooker, D.B., 1961, "Pressure patterns in grain drying system established by numerical methods", Transactions of the ASAE, 4, pp. 72-77.

Brooker, D.B., 1969, "Computing air pressure and velocity distribution when air flows through a porous medium and nonlinear velocity - pressure relationship exists", Transaction of the ASAE, 12, pp. 118-120.

Brooker, D.B., Bakker-Arkema, F.W., Hall, C.W., 1982, "Drying Cereal Grains", AVI Publishing Co., Westport, CT.

Bunn, J.M., Hukill, W.V., 1963, "Pressure pattern prediction for non-linear air flow through porous medium", Transactions of the ASAE, 6, pp. 32-36.

Haque, E., Chung, D.S., Forster, G.H., 1981, "Pressure and velocity field in airflow through packed bed of corn with fines non-Darcy flow conditions", Transactions of the ASAE, 5, pp. 1595-1604.

Khatchatourian, O.A., Savicki, D.L., 2004, "Mathematical modelling of airflow in an aerated store under non-uniform conditions", Biosystems Engineering, Vol.88, No.2, pp. 201-211.

Khatchatourian, O.A.; de Oliveira, F.A., 2006, "Mathematical modelling of airflow and thermal state in large aerated grain storage", Biosystems Engineering, Vol.95, No.2, pp. 159-69.

Liu, A., Joe, B., 1996, "Quality local refinement of tetrahedral meshes based on 8-subtetrahedron subdivision", Mathematics of Computation, Vol.65, No 215, pp. 1183-1200.

Maier, D.E., Moreira, R.G., Bakker-Arkema, F.W., 1992, "Comparison of conventional and chilled aeration of grains under Texas conditions", Applied Engineering in Agriculture, Vol.8, No 5, pp. 661-667.

Pierce, R.O., Thompson, T.L., 1975, "Airflow pattern in coaxial-shaped piles of grain", Transactions of the ASAE, 18, 946-949.

Puzzi, D., 1986, Abastecimento e armazenagem de grãos. [Provision and storage of grains.] ICEA, Campinas, Brasil

Ribeiro, C.A., Fortes, M., Hara, T., 1983, "Escoamento de ar em silos" [Airflow in silos.] Revista Brasileira de Armazenamento, Viçosa, Vol.891, No 20, pp. 28-31.

Scheidegger, A.E., 1960, "The physics of flow through porous media", 2nd ed., University of Toronto Press, Toronto

Segerlind, L.J., 1976, "Applied finite element analysis", J. Wiley and Sons Inc. New York, USA.

Shedd, C.K., 1953, "Resistance of grains and seeds to air flow", Agricultural Engineering, Vol.34, No 9, pp. 616-619

Weber, E., 1995, "Armazenagem Agrícola", [Agricultural storage.] Kepler Weber Industrial, Porto Alegre.

8. RESPONSIBILITY NOTICE

The authors are the only responsible for the printed material included in this paper.